

## Cytosolic calcium and membrane potential in articular chondrocytes during parabolic flight

Simon L. Wuest<sup>a,b</sup>, Geraldine Cerretti<sup>a,b</sup>, Jennifer Louise Wadsworth<sup>a,b</sup>, Cindy Follonier<sup>a</sup>, Karin F. Rattenbacher-Kiser<sup>a,b</sup>, Timothy Bradley<sup>c,d</sup>, Marcel Egli<sup>a,b</sup>, Fabian Ille<sup>a,b,\*</sup>

<sup>a</sup> Lucerne University of Applied Sciences and Arts, School of Engineering and Architecture, Institute of Medical Engineering, Space Biology Group, Hergiswil, Switzerland

<sup>b</sup> University of Zurich, Innovation Cluster Space and Aviation (UZH Space Hub), National Center for Biomedical Research in Space, Dübendorf, Switzerland

<sup>c</sup> University of Zurich, Faculty of Medicine, Institute of Anatomy, Zurich, Switzerland

<sup>d</sup> University of Zurich, Innovation Cluster Space and Aviation (UZH Space Hub), Air Force Center, Dübendorf, Switzerland

### ARTICLE INFO

#### Keywords:

Articular chondrocytes  
Membrane potential  
Cytosolic free calcium  
Gravity  
Parabolic flight  
Mechanosensitive ion channel

### ABSTRACT

Chondrocytes are the sole resident cells in articular cartilage, which line the articulating bones in joints allowing effortless movements. Chondrocytes are responsible for cartilaginous matrix synthesis, maintenance and degradation. Since these cells are frequently exposed to mechanical loading patterns, it is generally believed that chondrocytes require mechanical stimuli for adequate cartilage homeostasis. In this context, mechanosensitive ion channels are thought to be among the first instances in cellular mechanosensing. Prior studies showed that applied mechanical stimuli increase cytosolic free calcium and hyperpolarization of the cells' membrane potential. We used an adapted commercial plate reader during a parabolic flight to examine whether cytosolic free calcium and membrane potential are gravity-dependent. Our experiments showed that both cytosolic free calcium and membrane potential remain unchanged in response to short periods of increased or reduced gravity. Careful data analysis also revealed some pitfalls and shortcomings when using a commercial plate reader during a parabolic flight.

### 1. Introduction

Articular cartilage lines the articulating bones in joints, allowing near-effortless movement. To maintain healthy cartilage, frequent and adequate mechanical loading through an active physical lifestyle is essential. Prolonged mechanical unloading or overloading can lead to a pathological breakdown of articular cartilage and subsequent development of osteoarthritis (reviewed in Refs. [1,2]). Bed-rest studies, animal unloading models and clinical studies on astronauts returning from space have demonstrated that mechanical unloading leads to irreversible cartilage degradation (reviewed in Refs. [3–5]). Due to the limited self-healing properties of cartilage, joint replacement with an artificial prosthesis is often the only remaining measure to restore mobility and relieve pain in afflicted individuals.

Chondrocytes, the sole cell types found in articular cartilage, are responsible for matrix synthesis, maintenance and degradation (reviewed in Refs. [6–9]). Since chondrocytes are frequently exposed to mechanical loading patterns, it is generally believed that chondrocytes

require mechanical stimuli for adequate cartilage homeostasis (reviewed in Refs. [10–12]). However, to date the complex underlying mechanotransductional pathways are not fully understood. According to our current understanding, chondrocytes are thought to sense physical forces by multiple overlapping mechanisms (reviewed in Ref. [13]). Among other mechanisms, mechanosensitive ion channels (MSCs) are known to respond to mechanical forces, and are thought to play a key role in cellular mechanosensation (reviewed in Refs. [13–18]). This view is supported by pharmacological studies on mechanically stimulated cells, indicating that matrix synthesis depends on ion channel activity [19–22]. Moreover, specific ion channels are thought to play critical roles in the development of osteoarthritis (reviewed in Ref. [23]). Electrophysiological experiments on isolated chondrocytes suggest that MSCs could be among the first instances in mechanosensation. Exposure of isolated chondrocytes to osmotic challenges [22,24–30], fluid flow [31], compression [32], deformation [33,34] and aspiration [35] have been reported to trigger increased cytosolic free calcium. Furthermore, osmotic challenge [28], as well as prolonged pressure-strain loading

\* Corresponding author. Lucerne University of Applied Sciences and Arts, School of Engineering and Architecture, Institute of Medical Engineering, Obermattweg 9, CH-6052, Hergiswil, Switzerland.

E-mail address: [fabian.ille@hslu.ch](mailto:fabian.ille@hslu.ch) (F. Ille).

<https://doi.org/10.1016/j.actaastro.2022.01.016>

Received 8 October 2021; Received in revised form 6 January 2022; Accepted 13 January 2022

Available online 17 January 2022

0094-5765/© 2022 The Authors. Published by Elsevier Ltd on behalf of IAA. This is an open access article under the CC BY license

(<http://creativecommons.org/licenses/by/4.0/>).

(reviewed in Ref. [36]), lead to membrane hyperpolarization. Based on previous studies, we should expect a response in membrane potential to mechanical stimuli other than osmotic challenge.

Gravity is a very weak physical force at the cellular level, yet numerous cell types showed distinct adaptation processes to elevated or lowered gravity conditions (reviewed in Refs. [37–41]). Many studies have investigated the reaction of chondrocytes to various stimuli. However, their reaction to an altered gravity stimulus, specifically their early responses, remains unclear. Therefore, we recorded the cytosolic free calcium and membrane potential in isolated chondrocytes using a commercial plate reader during a parabolic flight. This promising approach allows measuring multiple samples in rapid succession. Previous studies already applied this technique on a neuronal cell line (SH-SY5Y) to monitor alterations in membrane potential and cytosolic free calcium concentration during parabolic flights [42,43]. Similarly, cytosolic free calcium has also been recorded in *Arabidopsis thaliana* cell cultures [44,45].

This study showed that cytosolic free calcium and membrane potential remained unchanged in response to the fast-changing gravity conditions during a parabola. The project also revealed some pitfalls and aspects scientists need to pay special attention to when using a commercial plate reader during parabolic flights.

## 2. Materials and methods

### 2.1. Chondrocyte cell culture

The human chondrocyte cell line C28/12 [46,47] was purchased from Merck (Schaffhausen, Switzerland) and expanded before the campaign (max. 5 passages). Passaged cells were periodically frozen and stored at  $-80^{\circ}\text{C}$  until use. Primary bovine articular chondrocytes were isolated from the distal interphalangeal (DIP) joints of slaughtered cattle (food chain), as described previously [48]. In brief, fresh joints were opened and the articular cartilage was removed using a scalpel. The cartilage was then chopped into millimeter-sized pieces, and chondrocytes were subsequently released from the matrix using two enzymatic digestion steps. First, the cartilage was incubated for 2 h in 0.1% pronase (Roche, Basel, Switzerland) and then overnight in collagenase II (Worthington, Lakewood, NJ, USA) which was adjusted to an activity of 600 U/ml. Both digestion steps were performed on a shaker at  $37^{\circ}\text{C}$ . The released cells were finally separated from remaining tissue pieces by a cell strainer and washed with phosphate-buffered saline (PBS; Gibco, Thermo Fisher Scientific). The suspended cells were immediately frozen and stored at  $-80^{\circ}\text{C}$  until use.

Frozen chondrocytes were transported on dry ice to the parabolic flight's site and seeded in commercial T75 flasks (culture area of ca.  $75\text{ cm}^2$ , cell culture treated) four days before the first flight. Cell culture

**Table 1**

The samples were split into multiple treatment conditions (listed in alphabetical order). Fixed cells were fixed with 4% formaldehyde for 10 min before staining and were used as a negative control. Untreated cells did not receive a special drug, and the wells were filled with KRH buffer only. The calcium-free ( $\text{Ca}^{2+}$ -free) buffer was identical to the KRH buffer, but the  $\text{CaCl}_2$  was replaced with 1 mM EGTA and NaCl increased to 134 mM. For the other treatment conditions, the respective drug was added to the KRH buffer after staining.

Treatment	Conc.	Action	Cells	Flight	Ref.
Amiloride	500 $\mu\text{M}$	Blocks ENaC, $\text{Na}^+/\text{H}^+$ and $\text{Na}^+/\text{Ca}^{2+}$ exchanges, L-type $\text{Ca}^{2+}$ channels and T-type $\text{Ca}^{2+}$ channels	Bovine, Human	73 <sup>rd</sup> : 3 75 <sup>th</sup> : 3	[57]
Apamin	4.9 $\mu\text{M}$	Blocks $\text{Ca}^{2+}$ -dependent $\text{K}^+$ channels (SK-channels)	Bovine, Human	73 <sup>rd</sup> : 3 75 <sup>th</sup> : 3	[57–59]
$\text{Ca}^{2+}$ -free	–	Blocks extracellular $\text{Ca}^{2+}$	Human	75 <sup>th</sup> : 1, 2	
Colchicine	10 $\mu\text{M}$ , >3 h	Inhibits tubulin polymerization	Bovine, Human	73 <sup>rd</sup> : 2 75 <sup>th</sup> : 1, 2	[34]
Cytochalasin D	20 $\mu\text{M}$ , >3 h	Disrupts actin	Bovine, Human	73 <sup>rd</sup> : 2 75 <sup>th</sup> : 1, 2	[34]
DMSO	0.25%	DMSO control	Human	75 <sup>th</sup> : 1, 2	
Fixed	4%, 10 min	Formaldehyde fixed cells (negative control)	Bovine, Human	73 <sup>rd</sup> : 1, 2 75 <sup>th</sup> : 1- 3	
$\text{Gd}^{3+}$	10 $\mu\text{M}$	Blocks extracellular $\text{Ca}^{2+}$ and MSCs	Bovine	73 <sup>rd</sup> : 1, 2	[25–27,31,34,57, 58,60]
GSK2193874	10 $\mu\text{M}$	Blocks TRPV4	Bovine, Human	73 <sup>rd</sup> : 1 75 <sup>th</sup> : 1	[61]
NPPB	100 $\mu\text{M}$	Blocks $\text{Cl}^-$ channels	Bovine, Human	73 <sup>rd</sup> : 3 75 <sup>th</sup> : 3	[62]
Ruthenium red	10 $\mu\text{M}$	Blocks CatSper1, KCNK3, RyR1, RyR2, RyR3, TRPM6, TRPM8, TRPV1, TRPV2, TRPV3, TRPV4, TRPV5, TRPV6, TRPA1, CALHM1, TRPP3, PIEZO	Bovine, Human	73 <sup>rd</sup> : 3 75 <sup>th</sup> : 2	[27,28,63]
Somatostatin	50 $\mu\text{M}$	Blocks voltage-dependent $\text{Ca}^{2+}$ channels	Bovine, Human	73 <sup>rd</sup> : 1 75 <sup>th</sup> : 1	[57]
TEA	20 mM	Blocks $\text{K}^+$ channels	Bovine, Human	73 <sup>rd</sup> : 3 75 <sup>th</sup> : 3	[64,65]
Thapsigargin	1 $\mu\text{M}$ , >1 h	Blocks SERCA (sarco/endoplasmic reticulum $\text{Ca}^{2+}$ -ATPase)	Bovine, Human	73 <sup>rd</sup> : 1, 2 75 <sup>th</sup> : 1, 2	[32]
Untreated	–	–	Bovine, Human	73 <sup>rd</sup> : 1- 3 75 <sup>th</sup> : 1- 3	

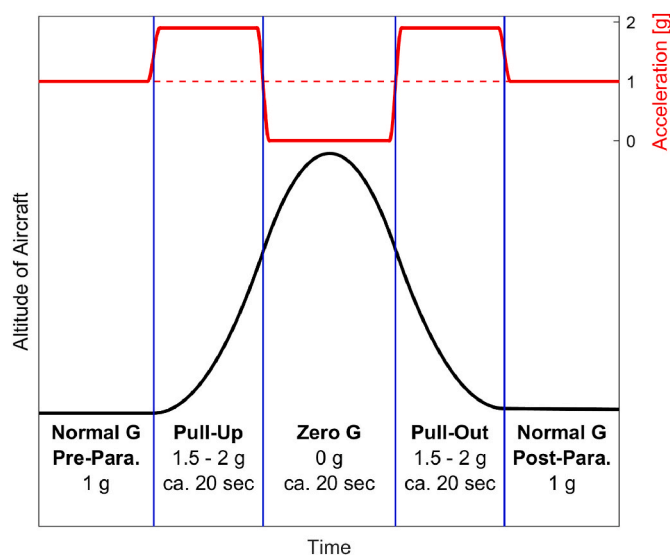


**Fig. 1.** Schematic illustration of the parabolic maneuver, which consists of three phases. First, from a steady horizontal flight, the aircraft is pulled-up ('Pull-Up'), resulting in a perceived acceleration between 1.5 and 2 g. Then, the aircraft is flown along a parabolic trajectory, such that it is in free-fall and microgravity is experienced ('Zero G'). Finally, the aircraft is pulled out from the parabola into steady horizontal flight ('Pull-Out'), resulting again in an acceleration of approximately 1.5–2 g.

medium contained DMEM buffered with 25 mM HEPES (PAN Biotech, Aidenbach, Germany) and supplemented with 10% fetal bovine serum (FBS; GE Healthcare, Pasching, Austria) and 1% penicillin streptomycin (Gibco, Thermo Fisher Scientific, Waltham, MA, USA). Fluorescent recordings were done in a Krebs-Ringer HEPES (KRH) buffer containing 130 mM NaCl, 5 mM KCl, 2 mM  $\text{CaCl}_2$ , 1.2 mM  $\text{MgSO}_4$ , 1.2 mM  $\text{KH}_2\text{PO}_4$ , 6 mM D-Glucose and 25 mM HEPES adjusted to pH 7.4.

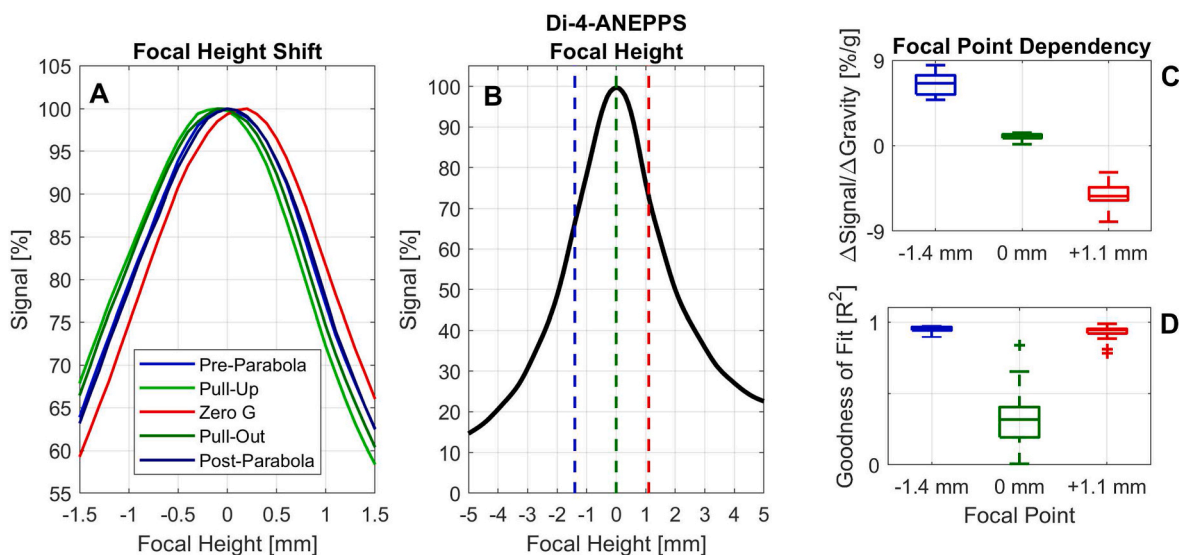


**Fig. 2.** Focal height curves were recorded during the different phases of a parabola on fixed and subsequently Di-4-ANEPPS-stained human chondrocytes (A). The focal height curves shift to the left during hypergravity (green lines) and to the right during low gravity (red line), which demonstrates an elastic displacement of the microplate. The focal height curve (B, black line) typically has a bell shape, with the maximum at the cell's level (green dashed line). The plate displacement can also be demonstrated by placing the focal point to the left (blue dashed line) or to the right (red dashed line) of the maximum. This results in a strong gravity-dependent signal change, which is proportional to the slope at focal point (C). The goodness of fit ( $R^2$ ) to the linear signal to gravity model increases to almost one, indicating a strong linear relation, when the optic's focal point is set out of focus (D). (For interpretation of the references to color in this figure legend, the reader is referred to the Web version of this article.)

## 2.2. Parabolic flight

The experiment was flown with an Airbus A310 operated by Novespace (Bordeaux, France) [49] during the 73<sup>rd</sup> and 75<sup>th</sup> parabolic flight campaigns of the European Space Agency (ESA). During each campaign, the experiments were flown on three flight days, on which 31 consecutive parabolas were flown per flight. The parabolic maneuver consists of three phases [50,51] (Figs. 1 and 5 and S1). First, from a steady horizontal flight, the aircraft is pulled up to an inclination of up to 50° for approximately 20 s ('Pull-Up' phase). During this phase, the samples are subjected to an acceleration of between 1.5 and 2 g. Then, the aircraft is flown along a parabolic trajectory, such that it is in freefall and microgravity is perceived inside the cabin for approximately 20 s ('Zero G' phase). During this period, the engine thrust is reduced to compensate for the air drag. Finally, at a declination of 42°, the aircraft is pulled out of the parabola into steady horizontal flight ('Pull-Out' phase). During this phase, which is also approximately 20 s long, the acceleration again increases to approximately 1.5–2 g.

## 2.3. Experimental design

### 2.3.1. 73<sup>rd</sup> ESA parabolic flight campaign

Bovine articular chondrocytes from seven different animals were thawed and seeded four days before the first flight and maintained in cell culture medium (Table S1). The cells from the seven animals were kept in separate culture flasks throughout the entire experiment and can therefore be regarded as biological replicas. Primary chondrocytes are known to acquire a spread-out morphology and to lose their phenotype in a standard monolayer culture [52–56]. Generally, after three to four passages the cells lose their capacity to produce an extra cellular matrix [56]. Therefore, cell culture time was reduced to a minimum with no prior passages for this study. Two days after seeding, the cells were transferred to 96-well plates (CellView Microplate, Greiner Bio-One, Frickenhausen, Germany; culture area of ca. 33 mm<sup>2</sup>/well, cell culture treated; 50'000 cells/well) and further incubated with cell culture medium until the day of flight. On the morning of each flight, the cells were washed with KRH buffer and stained with either 2 mM Fluo-4 and 2 mM

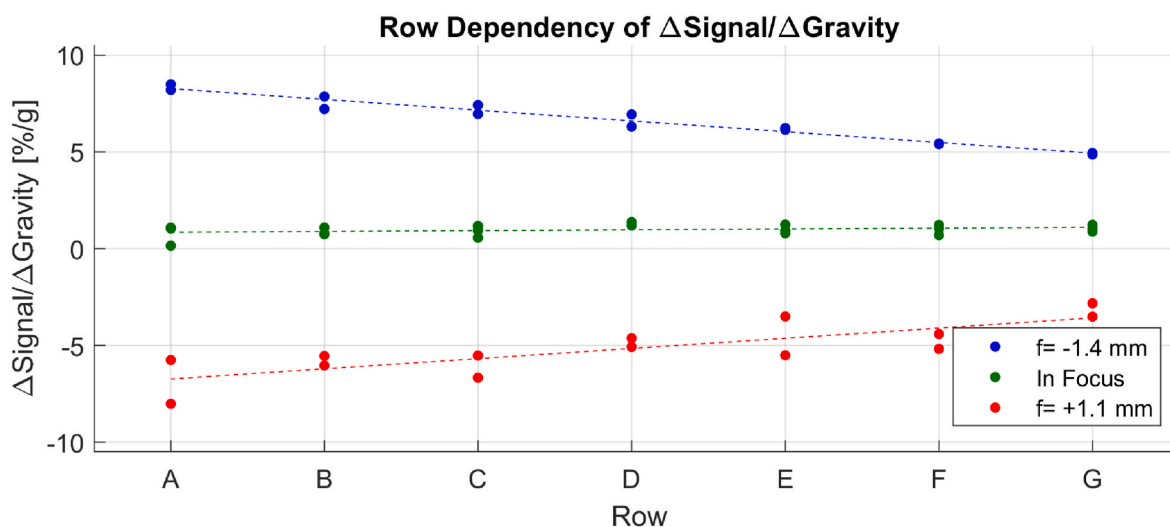


**Fig. 3.** Di-4-ANEPPS signal–gravity relation as a function of the microplate’s row (fixed human chondrocytes). The gravity sensitivity decreases from row A to row G if the focus is placed on the flanks of the focal curve (blue and red marks). This indicates that the microplate tilts, whereby row A experiences the largest and row H the least displacement. (The blank samples were in row H, and therefore, no data is available for this row). (For interpretation of the references to color in this figure legend, the reader is referred to the Web version of this article.)

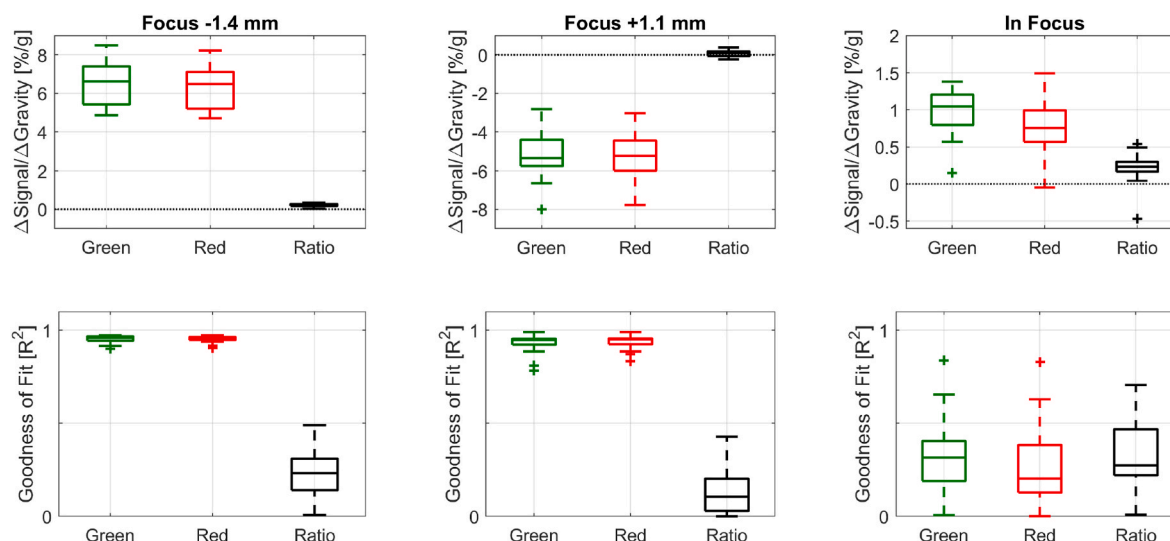


**Fig. 4.** Ratiometric measurement allows correcting for measurement errors, such as displacement of the microplate. The green (560 nm) and the red (>630 nm) signals in Di-4-ANEPPS-stained human chondrocytes (fixed cells) show a similar gravity dependency caused by the microplate movement under the gravitational load. If the optic’s focal point is placed out of focus, the green and red signals show an almost linear signal–gravity relation, as indicated by the high goodness of fit ( $R^2$ ). This measurement error can be reduced by computing the green to red ratio, resulting in a small gravity sensitivity and reducing the goodness of fit to the linear model.

Fura Red (co-staining; 1<sup>st</sup> flight) or with 4  $\mu\text{M}$  Di-4-ANEPPS (2<sup>nd</sup> and 3<sup>rd</sup> flights) dissolved in KRH buffer for 30 min in the dark (all stains from Invitrogen brand of Thermo Fisher Scientific, Dreieich, Germany). Subsequently, the cells were washed again with KRH buffer.

After staining, the samples were split into multiple conditions as listed in Table 1. Untreated cells received no special treatment, and the wells were filled with KRH buffer only. The fixed cells were fixed with 4% formaldehyde (Merck, Schaffhausen, Switzerland) for 10 min before staining and used as a negative control. Finally, all wells were completely filled with KRH buffer supplemented with the respective drug and sealed with foil (EASYseal, Greiner Bio-One, Frickenhausen, Germany). The number of biological (animals) and technical replicas is indicated in Table S3.

### 2.3.2. 75<sup>th</sup> ESA parabolic flight campaign

Expanded human chondrocytes (max. 5 passages) were thawed and seeded four days before the first flight and maintained in cell culture medium (Table S2). On the day before the flight, the cells were passaged to 96-well plates (CellView Microplate, Greiner Bio-One, Frickenhausen, Germany; culture area of ca. 33 mm<sup>2</sup>/well, cell culture treated; 50’000 cells/well) and further incubated with cell culture medium. On the morning of the flight, the cells were stained identically to the bovine samples. Subsequently, the human samples were also split into multiple conditions according to Table 1. Similarly, untreated sample wells were filled with KRH buffer only. The fixed cells were fixed with 4% formaldehyde for 10 min before staining and used as a negative control. The calcium-free ( $\text{Ca}^{2+}$ -free) buffer was identical to the KRH buffer, but the

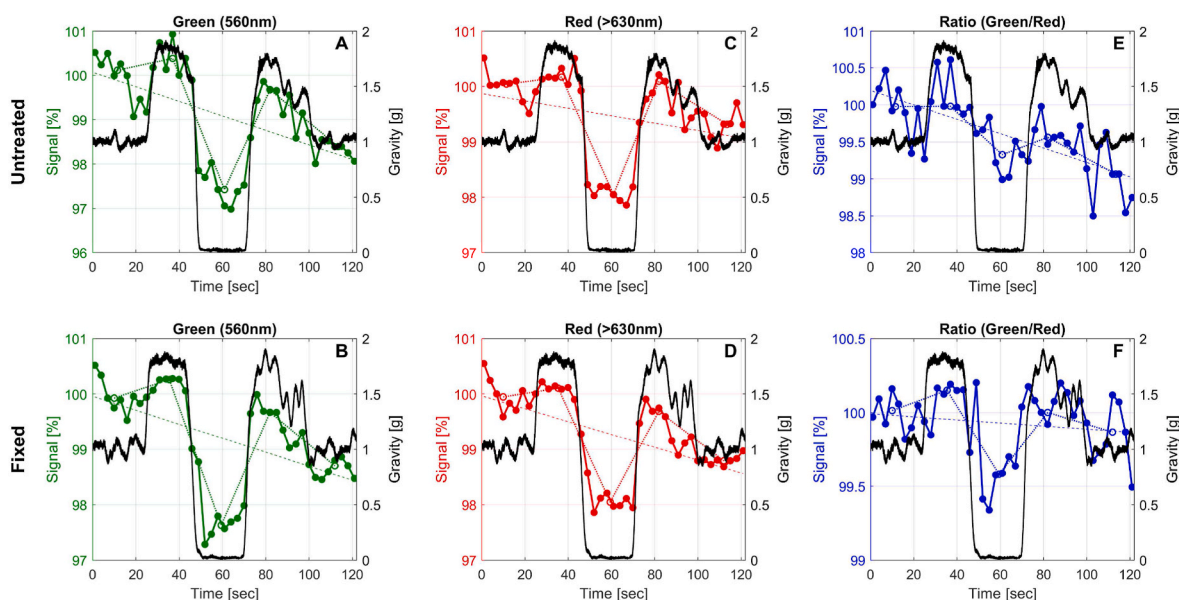


**Fig. 5.** Representative readings of Di-4-ANEPPS-stained untreated (top) and fixed (bottom) cells. The green (A, B) and the red (C, D) signal show a clear gravity dependency originating from the microplate displacement under the gravitational load. In addition, the signals show a photo-bleaching effect, indicated with the dashed lines. Computing the ratio of the green and red signals reduces these artefacts (E, F). Open marks indicate median values per flight phase and are connected by a dotted line.

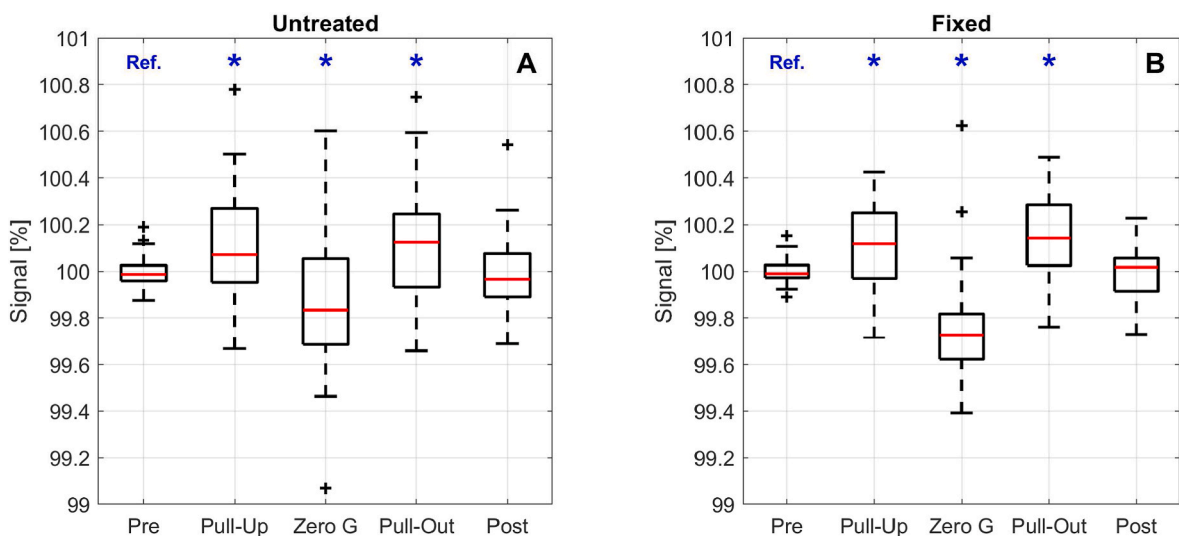


**Fig. 6.** Medians per flight phase shows a small gravity dependency that is similar in all treatment conditions, exemplified here with untreated (A) and fixed (B) samples. The ratiometric Di-4-ANEPPS signal from human chondrocytes was corrected for the photo-bleaching effect. As a similar pattern is observed in the fixed cells, where no biological activity is expected, the data includes some remaining error from the ratiometric correction. Asterisks indicate statistically significant differences compared to the 1 g phase just before the parabola. (Wilcoxon rank sum test,  $\alpha = 5\%$ ).

CaCl<sub>2</sub> was replaced with 1 mM EGTA and NaCl was increased to 134 mM. The number of technical replicas is indicated in Table S3.

#### 2.4. Hardware

The prepared sample were transferred into the aircraft shortly before take-off and maintained at 37 °C in a portable incubator (CellTrans 2018, Labotect, Göttingen, Germany) until the measurement were performed. Fluorescent measurements were taken with a modified commercial plate reader (PHERAstar FSX, BMG Labtech, Ortenberg, Germany; Table S4) with integrated temperature stabilization at 37 °C ( $\pm 0.1$  °C). Based on a previous design [43], the plate reader was

integrated in an aluminum flight rack to fulfill the current regulations and requirements for experiments on European parabolic flights (Figure S2). Fluo-4 and Fura Red co-stained cells were excited at 482 nm  $\pm$  16 nm and measured at 520  $\pm$  10 nm (Fluo-4) and 650  $\pm$  10 nm (Fura Red). The voltage-sensitive dye, Di-4-ANEPPS, was excited at 480  $\pm$  10 nm and measured at 560 nm  $\pm$  10 nm and >630 nm (long pass).

Recordings were started at normal gravity (1 g) approximately 30 s before parabola onset and continued for 120 s (approx. 20 s into normal gravity after the parabola). The plate reader had a special firmware modification and signal generator, which generated analog voltage impulses at the time points measurements were initiated. Signals from a gravity sensor (CXLO4GP3, Memsic, Milpitas, CA, USA) and the signal

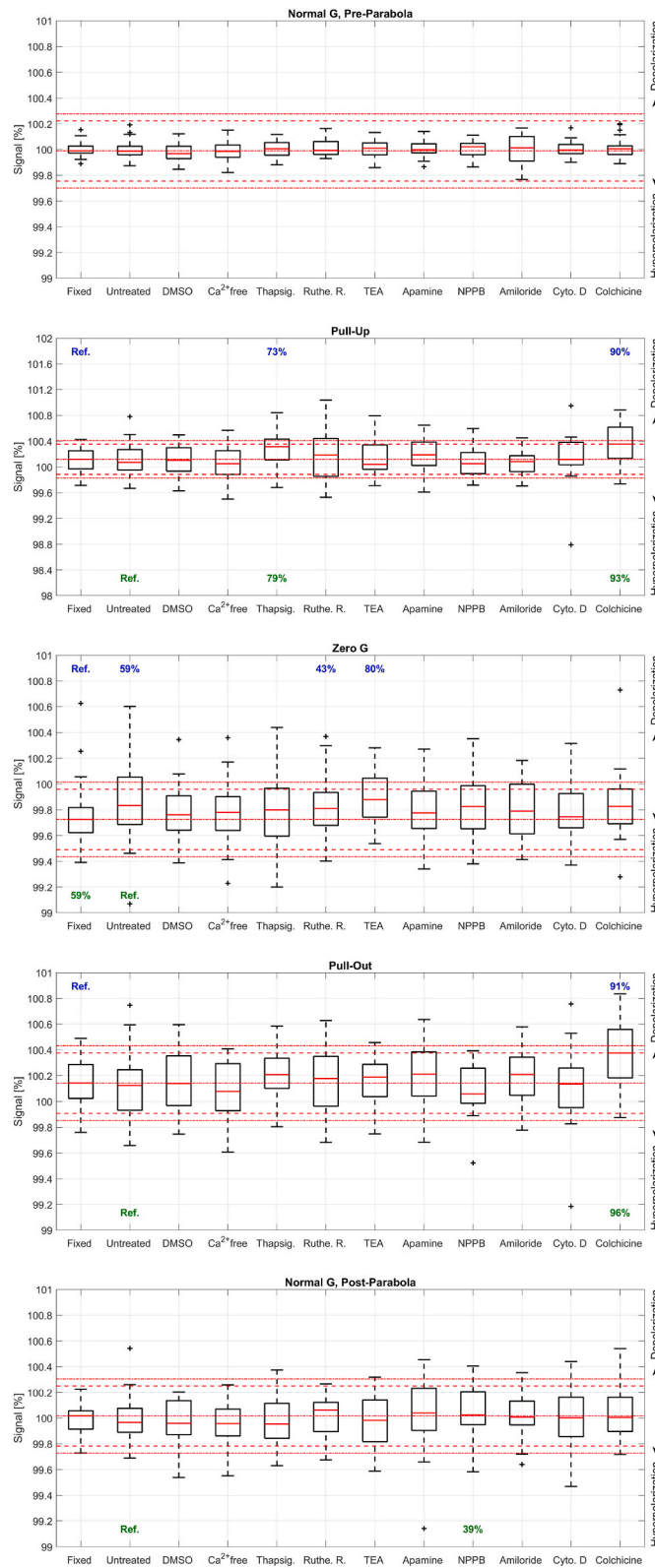


**Fig. 7.** Medians of the ratiometric- and photo-bleaching- corrected Di-4-ANEPPS signal from human chondrocytes per treatment condition and flight phase. If a statistically significant difference between either the fixed or untreated samples was computed (Wilcoxon rank sum test,  $\alpha = 5\%$ ), the power was estimated as well. (The power was computed using the means, standard deviations and the sample numbers of the two populations, assuming a Gaussian distribution.) The numbers indicate the computed power, if a treatment condition is statistically significantly different to either the fixed (blue, top numbers) or untreated (green, bottom numbers) condition. The horizontal red lines indicated the 90% confidence interval if three (dotted lines) or five (dashed lines) data points can be combined to one median value. (For interpretation of the references to color in this figure legend, the reader is referred to the Web version of this article.)

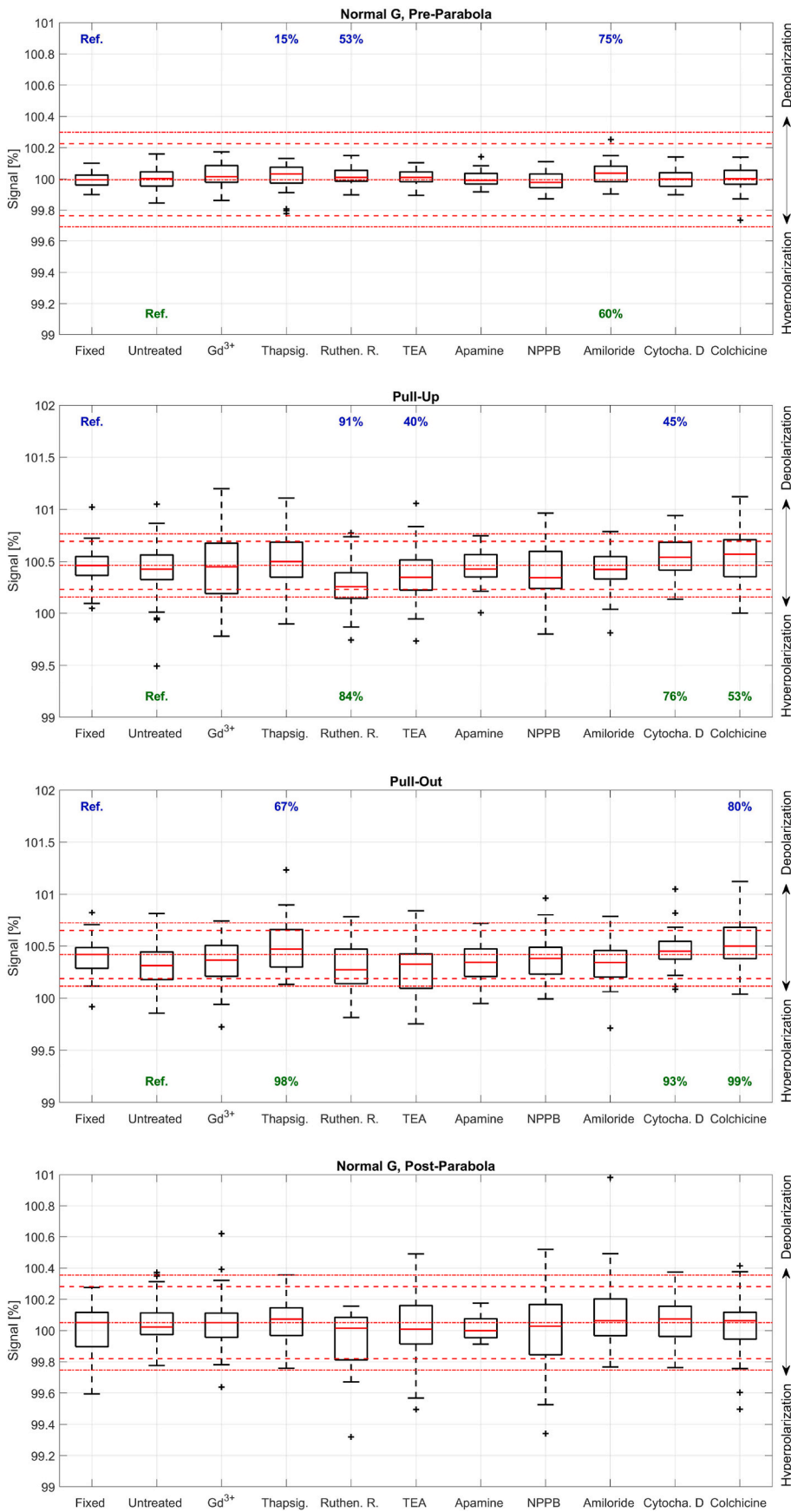


**Fig. 8.** Medians of the ratiometric- and photo-bleaching-corrected Di-4-ANEPPS signal from bovine chondrocytes per treatment condition and flight phase. Low gravity data was excluded. If a statistically significant difference between either the fixed or untreated samples was computed (Wilcoxon rank sum test,  $\alpha = 5\%$ ), the power was estimated as well. (The power was computed using the means, standard deviations and the sample numbers of the two populations, assuming a Gaussian distribution.) The numbers indicate the computed power if a treatment condition is statistically significantly different to either the fixed (blue, top numbers) or untreated (green, bottom numbers) condition. The horizontal red lines indicated the 90% confidence interval if three (dotted lines) or five (dashed lines) data points can be combined to one median value. (For interpretation of the references to color in this figure legend, the reader is referred to the Web version of this article.)

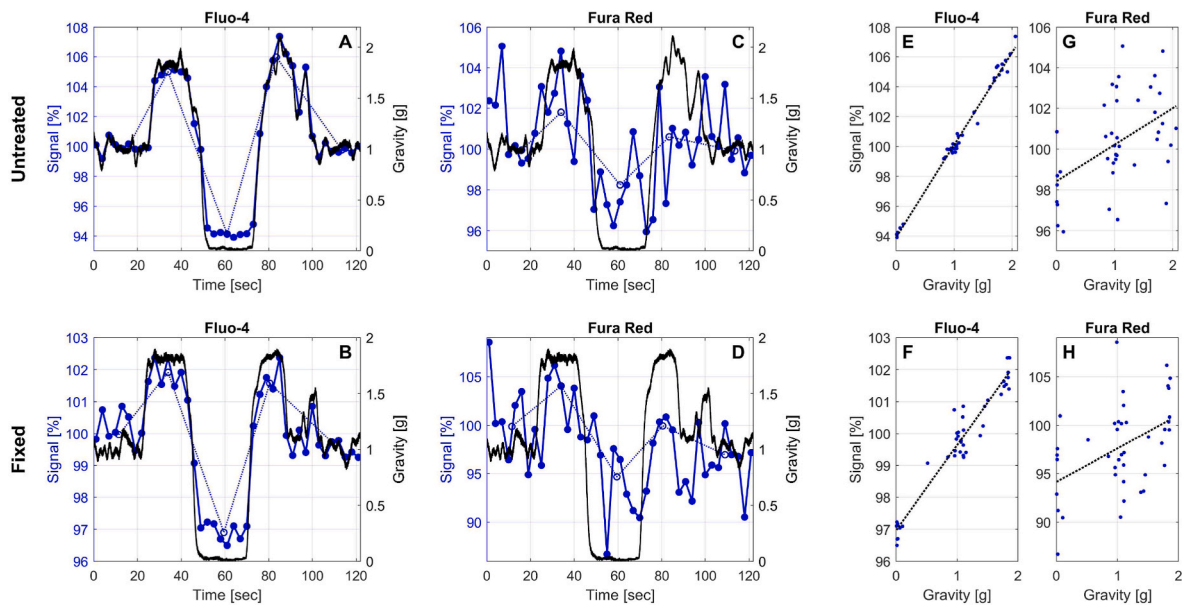


**Fig. 9.** Representative readings of Fluo-4 and Fura Red stained untreated (top) and fixed (bottom) cells. The Fluo-4 signal (A, B) shows a clear gravity dependency originating from the microplate displacement under the gravitational load. The signal shows a linear signal–gravity relation with a high goodness of fit (E, F). In contrast, the Fura Red signal (C, D) shows more “noise” with a small gravity dependency (G, H).

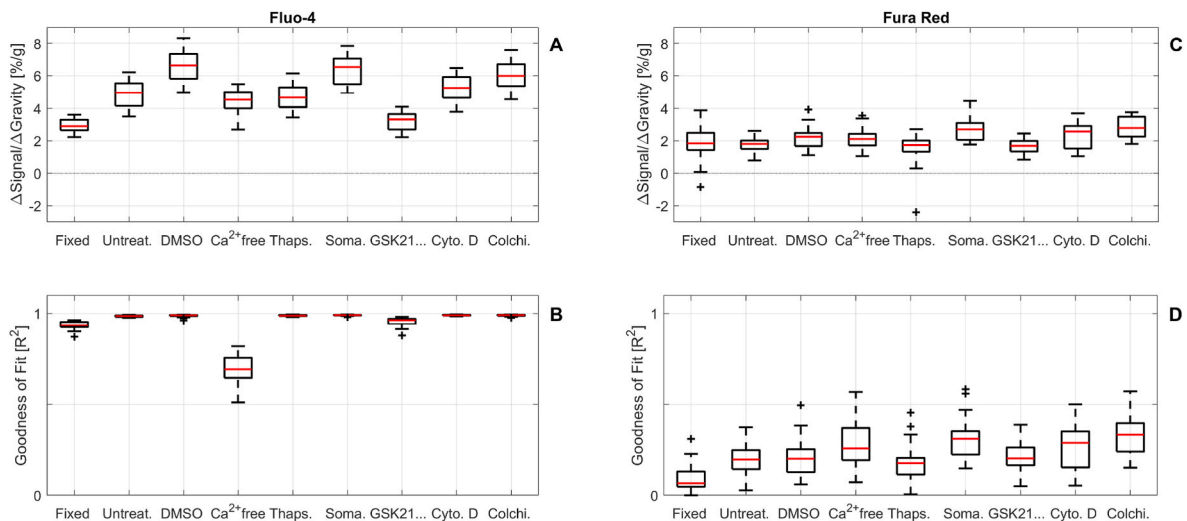


**Fig. 10.** In human chondrocytes, the signal to gravity relation shows a high linearity in the Fluo-4 signal as indicated by the high goodness of fit ( $R^2$ ; B). The steepness of the Fluo-4 signal–gravity relation is different among the treatment groups (A). In contrast, the slope of the Fura Red signal–gravity relation only shows minimal differences between the treatment groups (C). In addition, the low goodness of fit, indicates that the data poorly follows the linear model (D).

generator were recorded throughout the flight by a USB data acquisition device (USB-6001, NI, Austin, TX, USA). This allowed for alignment of the fluorescence measurements with gravity recordings post-flight.

## 2.5. Data analysis

Data acquisition and processing were done in a dedicated software program written in LabVIEW (2016). Data representation and statistical tests were performed using MATLAB (R2017b). Data processing was done according to the following workflow: (1) The acceleration data was smoothed and sectioned. Each data point was assigned to an individual parabola and a flight phase of a parabola (‘Normal G Pre-Parabola’, ‘Pull-Up’, ‘Zero G’, ‘Pull-Out’ and ‘Normal G Post-Parabola’). Data that could not be assigned to a specific flight phase was considered to have occurred in a transition phase (e.g., the aircraft transitioned from ‘Pull-Up’ into ‘Zero G’ when initiating the parabola.) (2) The background

signal recorded in the blank wells (row H) was deducted from the fluorescent values (blank correction). (3) Each fluorescent value was matched with the corresponding gravity reading and assigned a parabolic flight phase. (4) For each sample, the fluorescent values were normalized to the average value of the normal gravity phase just before the parabola (‘Normal G Pre-Parabola’). (5) For ratiometric measurements (Di-4-ANEPPS), the ratio of the corresponding data points from both colors was computed. Further data processing (computation of median, gravity sensitivity, etc.) is explained in detail below. Also, Di-4-ANEPPS showed a signal drop over time (photo bleaching), which was corrected by the linear component (see below for detailed remarks).

Statistical significance was tested using the non-parametric Wilcoxon rank sum test.  $P$ -values below 5% were considered statistically significant. The power between two populations (probability that the null hypothesis was correctly rejected) was estimated by generating  $10^5$  times two Gaussian populations with equal means, standard deviations

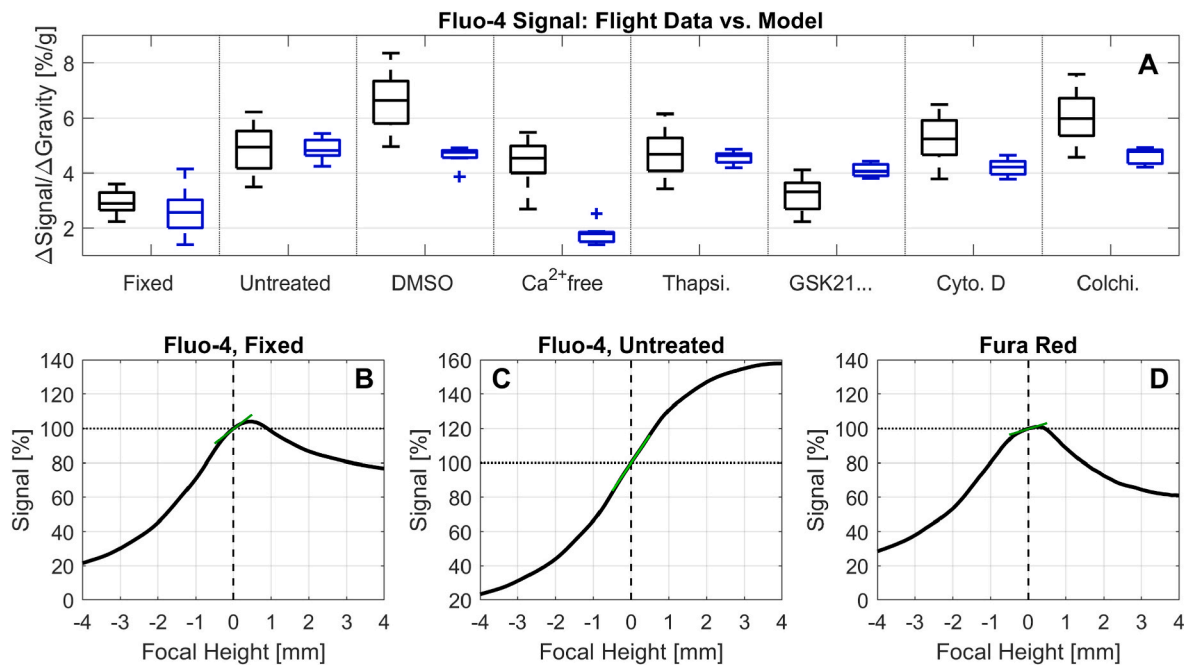


**Fig. 11.** In human chondrocytes, the Fluo-4 signal shows a high linearity to gravity (Fig. 10), with different signal to gravity sensitivity among the treatment groups (A, black boxes). This can largely be explained by the slope at the focal point in the focal height curve (green lines). The autofluorescence of the foil, which was used to close the microplate, can be seen in the Fluo-4 signal. In fixed samples, this shifted the maximum toward the foil (B). In untreated cells, where the signal is low in steady state, the foil's autofluorescence becomes dominant (C). This leads to different steepness of the focal height curve around the focal point (level of the cells) among the treatment groups. By multiplying this steepness with an assumed plate displacement of 0.15 mm/g, it largely explains the different signal to gravity sensitivity (A, blue boxes). The focal height curve of Fura Red was similar in the different treatment groups (D). (Focal height curves were normalized to 100% at the focal point). (For interpretation of the references to color in this figure legend, the reader is referred to the Web version of this article.)

and sample numbers. The two artificial populations were also tested for significant differences using the Wilcoxon rank sum test ( $\alpha = 5\%$ ). Power was finally computed by the ratio of significant differences over total runs.

### 3. Results

Primary bovine articular chondrocytes, as well as human chondrocytes, were exposed to altered gravity conditions during the 73<sup>rd</sup> and 75<sup>th</sup> ESA parabolic flight campaigns, respectively. In this special flight maneuver [50,51] (Figs. 1 and 5 and S1), the pilots first pull up the aircraft ('Pull-Up' phase), which creates hypergravity. Then the aircraft is flown along a parabolic trajectory, bringing the aircraft into freefall, and exposing its payload to microgravity ('Zero-G' phase) for about 20 s. Finally, the aircraft is pulled out of the parabola into horizontal flight again ('Pull-Out' phase), which is again associated with hypergravity. During the 'Pull-Up' and 'Pull-Out' phases, gravity increases to approximately 1.5–2 g, also for about 20 s.

Just before the flights, chondrocytes were split into multiple conditions as listed in Table 1 and stained either with the calcium-sensitive dyes Fluo-4 and Fura Red (co-staining) or the voltage-sensitive dye Di-4-ANEPPS. Relative fluorescence units (RFU) were measured with a modified commercial plate reader. Readings were started under normal gravity conditions (1 g) just before a parabolic maneuver, continued during the parabola and terminated again under normal gravity after the maneuver.

#### 3.1. Hardware performance

The data on the bovine chondrocytes (73<sup>rd</sup> ESA parabolic flight) showed a signal increase during the hypergravity phases ('Pull-Up' and 'Pull-Out') and a large signal drop during the microgravity phase ('Zero G') on all color channels and samples (Figure S3). This was also seen in the fixed cells where no change was expected (negative control).

Plotting the fluorescent signals against gravity revealed an approximately linear behavior between 0.5 and 2 g, and a "kink" at approximately 0.5 g, such that low-gravity samples showed a lower fluorescent value (Figure S4). Detailed analysis by BMG Labtech (the plate reader manufacturer) revealed that the photomultiplier tubes (PMTs) had begun rotating out of their position under low-gravity conditions. This explained the "kink" in the fluorescence-to-gravity relation and the fluorescent signal drop under low gravity. Because of the specific alignment of the PMTs, the displacement of the two PMTs was not equal. This caused the different magnitudes of signal drop in the two color channels. The linear range between 0.5 and 2 g suggested that the microplate was slightly displaced and tilted under the varying gravity load. However, we had insufficient data to conclusively prove or exclude this speculation. We had the unique opportunity to re-fly the experiment on the 75<sup>th</sup> ESA parabolic flight. Before the flight, the mounting of the PMTs was modified by BMG Labtech, such that they would not move under varying gravitational loads. To include more quality controls to better assess hardware performance, we used a standardized human chondrocyte cell line (C28/I2) and thereby lost the biological variability of primary bovine chondrocytes from multiple animals.

Recordings with the upgraded plate reader showed that the fluorescent signals plotted against gravity have an approximately linear relation for all color channels (Figure S5). This indicated that the new PMTs' mounting was successful, but that there was still an elastic distortion in the optical setup. Focal height curves were recorded on fixed cells (in which no change was expected), during the different phases of a parabola. This demonstrated an elastic displacement of the microplate (Fig. 2). The microplate moved down during hypergravity and moved up during low gravity, with a displacement of approximately 0.1–0.2 mm/g. The same behavior was confirmed by placing the focal point to the left or to the right of the maximum in the focal height curve. The normal focal height curve had a bell shape with the maximum at the level of the cells. By placing the focal point on the flank to the left or to the right of the maximum, the microplate displacement resulted in a

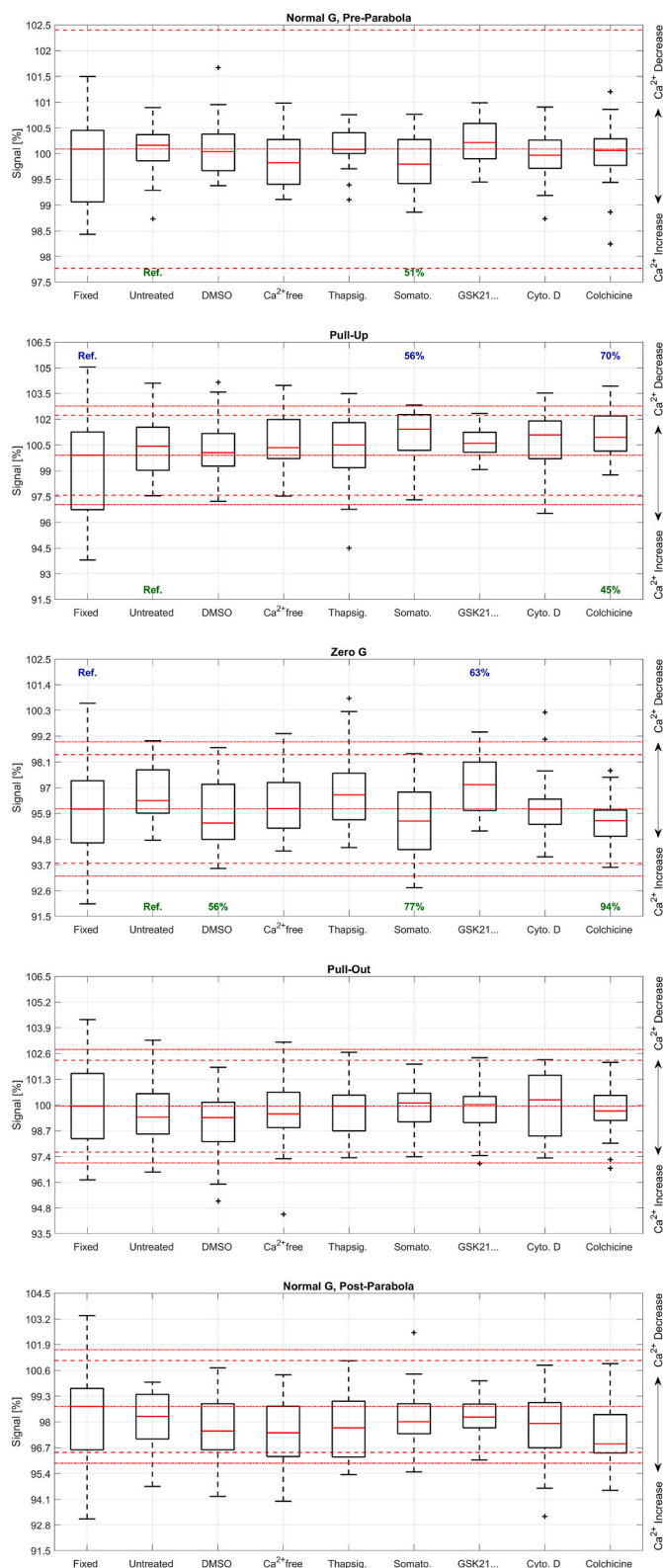


**Fig. 12.** Medians of the Fura Red signal from human chondrocytes per treatment condition and flight phase. If a statistically significant difference between either the fixed or untreated samples was computed (Wilcoxon rank sum test,  $\alpha = 5\%$ ), the power was estimated as well. (The power was computed using the means, standard deviations and the sample numbers of the two populations, assuming a Gaussian distribution.) The numbers indicate the computed power if a treatment condition is statistically significantly different to either the fixed (blue, top numbers) or untreated (green, bottom numbers) condition. The horizontal red lines indicated the 90% confidence interval if three (dotted lines) or five (dashed lines) data points can be combined to one median value. (For interpretation of the references to color in this figure legend, the reader is referred to the Web version of this article.)

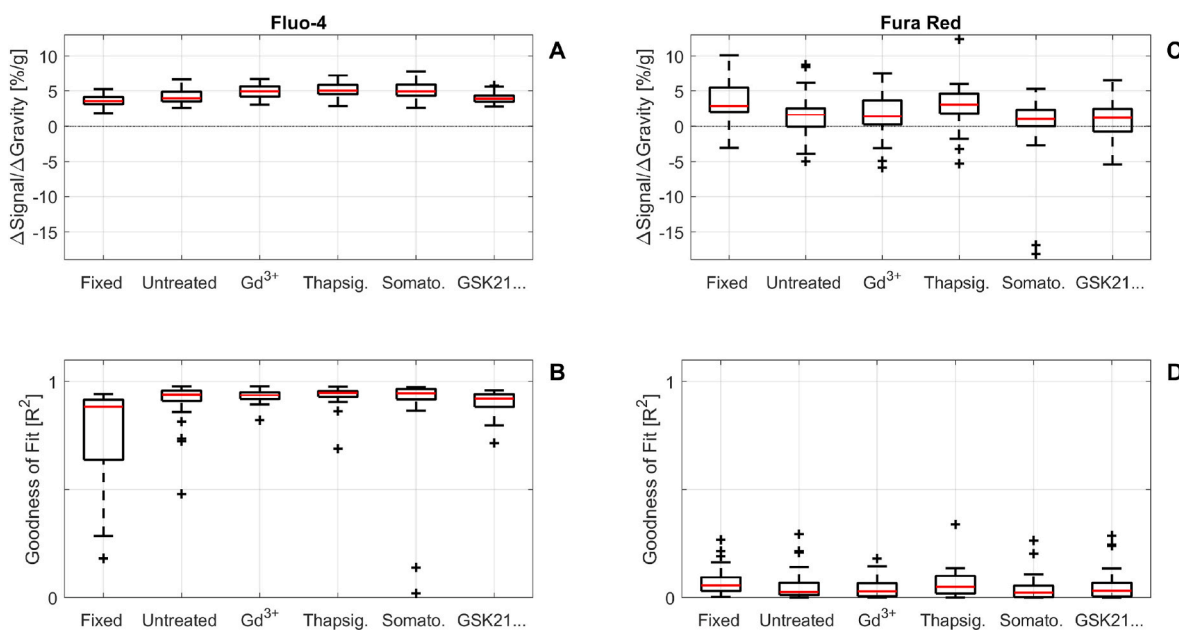


**Fig. 13.** Bovine chondrocytes overall show a similar picture to the human chondrocytes. However, the low gravity data has been removed, which could be the reason for some difference. The signal to gravity relation also shows a high linearity in the Fluo-4 signal as indicated by the high goodness of fit ( $R^2$ ; B). The steepness of the Fluo-4 (A) and Fura Red signal (C) to gravity is comparable among the treatment groups. Similar, Fura Red has a low goodness of fit, to the linear model (D).

small shift along the flank. This became visible as a strong gravity-dependent signal change. The slope of the signal–gravity relation was proportional to the slope of the focal height curve at the point at which the focus was set (Fig. 2). This data confirmed that the plate displacement was around 0.1–0.2 mm/g. By plotting the slope of the signal–gravity relation as a function of the microplate’s row (A–G), it became clear that the plate displacement was row-dependent (Fig. 3). This indicates that the microplate also tilted, with row A experiencing the greatest displacement and row H the least displacement. However, the microplate displacement described above could largely be compensated for by using ratiometric measurements, as discussed below.

### 3.2. Membrane potential

Di-4-ANEPPS exhibits a spectral emission shift in response to changing membrane potential [66]. The emission maximum shifts to shorter wavelengths upon depolarization and to longer wavelengths upon hyperpolarization [66]. In bovine and human chondrocytes, the steady-state emission maximum is at roughly 595 nm, (excited at 480 nm; Figure S6). A membrane potential shift to a more positive potential (depolarization) therefore results in a signal increase at 560 nm (green signal) and a signal decrease at >630 nm (long pass, red signal). Thus, signal changes in opposite directions indicate a true change in membrane potential. On the other hand, signal changes in the same direction indicate signal distortion related to the measurement setup, such as displacement of the microplate or photo bleaching. Therefore, computing the ratio of the green (560 nm) over the red (>630 nm) signal allowed us to correct for such measurement errors. The clear signal–gravity relation seen in the two colors could effectively be reduced by computing the ratio between them (Fig. 4 and S5).

The blank-corrected and ratiometric Di-4-ANEPPS signals showed variability around the mean, little gravity dependency and an almost linear signal drop (Fig. 5). To correctly interpret the signal, separation of these overlapping effects was required. The signal drop could be attributed to a photo-bleaching effect and was unlikely to be true hyperpolarization. Similar signal drops were observed in the lab and at 1 g in flight (before the parabolas). Also, no difference was seen when measuring in ‘plate mode’, in which the plate moves during the measurements from well to well; or in ‘well mode’, in which the plate only

moves before or after measurements (Figure S7). We attribute the difference in signal decay between the untreated and fixed samples to different chemical interactions of the dye with the fixed samples. To eliminate the photo-bleaching effect, the data was corrected by the linear component of the signal decay for further analysis.

To increase signal precision, we computed the medians for every flight phase (‘Normal G Pre-Parabola’, ‘Pull-Up’, ‘Zero G’, ‘Pull-Out’ and ‘Normal G Post-Parabola’). Data points that could not be assigned to a specific flight phase were considered to be from a transition phase and were excluded. The number of data points that could be included and essentially contribute to each median value is illustrated in Figures S8 to S11. For the ‘Normal G Pre-Parabola’, ‘Pull-Up’ and ‘Zero G’ phases most often five or more data points could be included, but never fewer than three data points. The ‘Pull-Out’ and ‘Normal G Post-Parabola’ phases appeared to be more problematic, as the gravity level was often unstable (Figure S1); in several conditions, only one or two data points could be included. To better understand the variability of the data, recordings of untreated and fixed samples (acquired in the lab on the ground) were smoothed with a median filter including either three or five data points, and the difference between the 5<sup>th</sup> and the 95<sup>th</sup> percentiles was computed. This represents the range in which a median value could appear by chance with 90% probability (Fig. 7).

Comparing the median of the photo bleaching-corrected data from all flight phases showed a small gravity dependency that was similar in all treatment conditions (Fig. 6). As a similar pattern was observed in all treatment conditions, including the fixed cells in which no biological activity was expected, the data included some residual error from the ratiometric correction. To assess for differences among the different treatment groups, the medians were compared separately by flight phase. The Wilcoxon rank sum test ( $\alpha = 5\%$ ) yielded a statistically significant difference in the human chondrocytes between the fixed and the untreated cells during the ‘Zero G’ phase (Fig. 7). However, compared to the 5%–95% confidence interval, most of the data was well within that range. In addition, the power (computed from the means, standard deviations and the sample numbers of the two populations) was rather low (approx. 59%). Segmenting the data by flight day, a statistically significant difference was only seen in one flight day. Statistically significant differences compared to either the fixed or untreated samples were also identified for thapsigargin, ruthenium red, TEA, colchicine and NPPB.

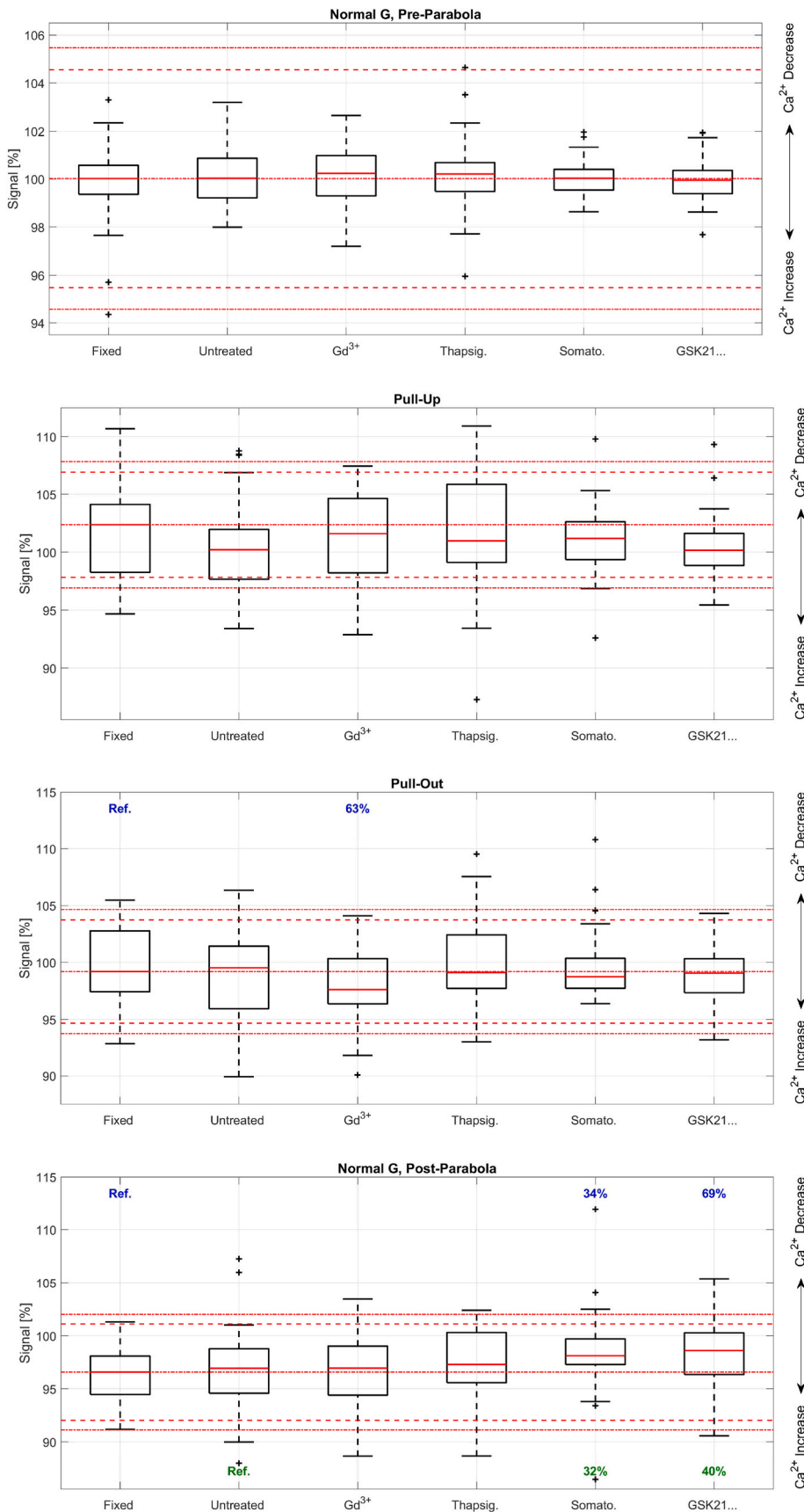


**Fig. 14.** Medians of the Fura Red signal from bovine chondrocytes per treatment condition and flight phase. Low gravity data was excluded. If a statistically significant difference between either the fixed or untreated samples was computed (Wilcoxon rank sum test,  $\alpha = 5\%$ ), the power was estimated as well. (The power was computed using the means, standard deviations and the sample numbers of the two populations, assuming a Gaussian distribution.) The numbers indicate the computed power if a treatment condition is statistically significantly different to either the fixed (blue, top numbers) or untreated (green, bottom numbers) condition. The horizontal red lines indicated the 90% confidence interval if three (dotted lines) or five (dashed lines) data points can be combined to one median value. (For interpretation of the references to color in this figure legend, the reader is referred to the Web version of this article.)

However, the power was greater than 80% only for colchicine during the two hypergravity phases (drug actions are summarized in Table 1). For the bovine primary cells, all low-gravity data had to be excluded as the PMTs had rotated out of place during this phase (see “Hardware performance” section). Statistically significant differences with low power in comparison to either the fixed or untreated samples were present for thapsigargin, amiloride and TEA (Fig. 8). The data also suggests that bovine chondrocytes hyperpolarize during the ‘Pull-Up’ phase when exposed to ruthenium red. Furthermore, the data indicates that bovine chondrocytes depolarize under hypergravity if incubated in cytochalasin D or colchicine. Also, we analyzed the local signal changes within flight phases. We could find no directionality or pattern distinct from the fixed samples (negative control group) for either the human or bovine chondrocytes (Figure S12 and S13).

### 3.3. Cytosolic free calcium

We assessed changes in cytosolic free calcium by co-staining the cells with Fluo-4 and Fura Red to take advantage of ratiometric measurements. The Fluo-4 signal (excited at 482 nm and measured at 520 nm) increases with increasing calcium concentration. In contrast, the Fura Red signal (excited at 482 nm and measured at 650 nm) decreases with increasing calcium concentration. Our measurements showed distinct signal patterns for the two dyes (Fig. 9). The Fluo-4 signal closely followed the gravitational load and showed a linear signal–gravity relation (Fig. 9). The high goodness of fit to the linear model indicated that the signal change was of technical origin. Interestingly, the slope of the signal–gravity relation was different for the various treatment conditions (Fig. 10). This data was not confirmed by the Fura Red signal, which only showed a small gravity dependency with minimal difference between the treatment groups (Fig. 10). Post-flight analysis showed that these observations could be explained by the slope of the focal height curve at the focal point and the already described microplate displacement (Fig. 11). In steady state, untreated cells maintained a low cytosolic calcium concentration and showed a weak Fluo-4 signal. In these samples, the autofluorescence of the foil that was used to seal the microplate could already be seen in the focal height curve. In contrast, in fixed cells, the Fluo-4 signal was strong and the focal height curve showed the more typical bell shape, with the maximum shifted toward the foil (Fig. 11). Computing the slope of the focal height curve at the focal point and assuming a microplate displacement of 0.15 mm/g explained the signal–gravity relations (Fig. 11). In contrast, the focal height curve of the Fura Red signal showed a bell shape in all samples. Therefore, the signal was less distorted by the displacement of the microplate (Fig. 11).

In the human chondrocytes, the change in the Fluo-4 signal merely indicated the displacement of the microplate due to the gravitational load. The almost perfect linearity between the signal and the gravitational load ( $R^2$  close to 1) was a strong indicator that the signal was of technical origin (Fig. 10). We were therefore unable to identify a gravity-dependent Fluo-4 signal originating from the cells. The  $Ca^{2+}$ -free condition was distinct from the other conditions, as it showed lesser goodness of fit ( $R^2$ ) to the linear model. In this condition, the Fluo-4 signal continuously dropped over time, which was independent of the flight phases and explained the lower goodness of fit ( $R^2$ ). In contrast, the Fura Red signal exhibited little gravity dependency and a minor photo-bleaching effect in all conditions. By comparing the medians of the various conditions in each flight phase, the Wilcoxon rank sum tests ( $\alpha = 5\%$ ) revealed some statistically significant differences compared to either the fixed (negative control) or untreated samples (Fig. 12). However, most of the data remained within the range one would expect randomly with a 90% probability. Also, the estimated power was low. It was only above 80% when comparing the untreated and colchicine-treated samples during ‘Zero G’.

A similar picture was seen in the bovine chondrocytes. The Fluo-4 signal showed high linearity to the gravitational load (Fig. 13).

However, the fixed samples were not in line with the other samples. The goodness of fit was lower and had greater variability. The reason for this remained unclear and could be the result of excluding the low-gravity data. Comparison of the medians of the Fura Red signal in the different flight phases showed statistically significant differences between the fixed and  $Gd^{3+}$  treated samples during ‘Pull-Out’ as well as in the somatostatin- and GSK2193874-treated samples compared to both the fixed and untreated samples after the parabola (Fig. 14). However, the power was less than 70% for all detected differences. Furthermore, analysis of the local signal change within a flight phase showed no directionality or pattern for either the human or bovine chondrocytes (Figures S14 to S17). (Again, ‘Zero G’ data was removed in the bovine samples because the PMT rotated away during this period.)

## 4. Discussion and conclusion

The mechanical environment of parabolic flights, including vibrations and alternating gravitational load, make electrophysiological recordings that require micromanipulations very challenging (reviewed in Ref. [40]). On the other hand, optical systems proved more robust and easier to use on microgravity platforms [40]. The advantages of ready to use commercial plate readers and the relatively small modifications for parabolic flights make them a tempting option. High-throughput plate readers allow for measuring multiple samples in rapid succession, providing high quality components with high signal sensitivity. In combination with a large selection of fluorescent dyes, which work well on most cell types, plate readers are a versatile and powerful tool. However, plate readers were developed for lab use under normal gravity, and simply loading them into an aircraft can provide a number of pitfalls. The here-described experiment taught us some important lessons, demonstrating the limitations and required quality controls when using plate readers on microgravity platforms.

From the fixed cells’ data, we may draw the following conclusions. Firstly, the microplate is slightly displaced under the gravitational load in the range of 0.1–0.2 mm/g (Fig. 2). Secondly, the microplate displacement is row dependent, indicating microplate tilt. Thereby, row A experiences the largest and row H the least displacement (Fig. 3). Thirdly, the focal height curve’s slope at the focal point has a large impact on the readout (Figs. 2 and 11). Due to the small microplate displacement, the readout follows the focal height curve, which one could misinterpret as an actual signal change. Ideally, the focal height curve has a bell shape, with the maximum at the cell’s level. In this case, the slope would be horizontal and provide little signal distortion. In our calcium recordings, the autofluorescence of the foil, which closed the microplates, interfered with the focal height curve (Fig. 11). For Fura Red, the maximum shifted toward the foil, such that the slope became positive at the focal point. In Fluo-4, the impact was more severe when the signal was weak (untreated cells), completely altering the focal height curve. As adhesive foils and/or lids are required to close the microplate for parabolic flights, one must assess their influence on the fluorescent signal and the focal height curve.

Ratiometric measurements can compensate for the signal change caused by the microplate displacement, if three rules are respected (Fig. 4). Firstly, to detect signal changes caused by moving optical part, the signals of the two colors must respond in opposite direction to the examined variable (e.g., calcium or membrane potential). For instance, the Fluo-4 signal increases with increasing cytosolic calcium concentration, but the Fura Red signal decreases with increasing calcium concentration. If this is not possible, the signal should at least be compared to a fluorescent signal that is independent of the examined variable. Secondly, the focal height curve’s slope at the focal point should be similar for the two colors. Otherwise, the ratiometric correction will be insufficient, which could be misinterpreted as a true signal. Thirdly, the recording for the two colors should be simultaneous. In our experiment, these rules were respected using Di-4-ANEPPS, and the ratiometric correction was indeed successful. However, the foil’s

autofluorescence violated the second rule in the calcium measurements. The Fluo-4 signal's steep slope at the focal point leads to a strong gravity dependency for which the Fura Red signal could not compensate (Figs. 10 and 11). Therefore, a ratiometric correction was not possible anymore, as it would have been insufficient.

Ultimately, as the ratiometric correction is never perfect, the signal from the samples should always be compared to a negative control for which no change is expected (Fig. 6). Furthermore, one should keep in mind that the focal curve might change between different test conditions, leading to a misinterpretation of the results (Fig. 11).

Overall, we conclude that the membrane potential and the cytosolic free calcium in bovine (from 0.6 to 1.8 g) and human (from 0 to 1.8 g) chondrocytes is not gravity dependent in the examined gravity and time range. Even though the nonparametric Wilcoxon rank sum test computed some statistically significant differences ( $\alpha = 5\%$ ), they were small, with low power, and the signals remained well within the expected variability. Therefore, the statistically significant differences were not convincing, and the findings might well be coincidental. For instance, the statistically significant difference in the human chondrocytes between the fixed and the untreated cells during the 'Zero G' phase (Fig. 7) was only seen in one out of two flight days, and most of the data was well within the 5%–95% confidence interval. These results support the idea that a small p-value might not necessarily indicate a true finding.

The Fluo-4 signal's strong gravity dependency, which could be easily misinterpreted as a true signal, merely represented the microplate's displacement under the gravitational load (Fig. 10). Therefore, together with the Fura Red data, we were unable to identify a gravity dependent change in cytosolic free calcium. This finding agrees with our second approach using the genetic calcium indicator CaMPARI [67].

The colchicine treatment was an exception in comparison to the other conditions because it showed convincing differences in human (Fig. 7) and bovine (Fig. 8) chondrocytes during hypergravity. The data suggest that colchicine-treated chondrocytes depolarize (positive membrane potential change) when exposed to hypergravity. Colchicine inhibits tubulin polymerization and eventually results in a disrupted tubulin network (Figure S18) [34,68]. This suggests that the membrane potential in chondrocytes only becomes sensitive to gravity when the stabilizing tubulin network is disrupted. In a previous experiment, we found that exposure to parabolic flights does not disrupt or reorganize the tubulin network in bovine articular chondrocytes [69]. This could explain why untreated chondrocytes showed no electrophysiological response in this study.

The study presented here demonstrated that using standard lab equipment, which was designed for use under normal gravity, requires careful implementation and sufficient quality control. Our results raise some questions on the validity of previous experiments performed with plate readers during parabolic flights [42,43,70]. In conclusion, we may formulate some guidelines and questions that should be addressed when using plate readers in parabolic flights.

- How much does the microplate move under gravitational load? Does the resulting signal distortion render the experiment invalid?
- Is there a row or column dependency that should be considered?
- The focal height curve's slope at the focal point has a large impact on the readout if the microplate moves slightly. Therefore, this should be assessed.
- What is the influence of foils, lids and other components in the optical path on the fluorescent signal and the focal height curve? Consider that autofluorescence might only be detected if the actual fluorescent signal is weak.
- Fluorescence measurements should only be done ratiometrically or at least in reference to a control signal.
- Ratiometric measurements require that (1) the two colors change in opposite direction in response to the examined variable; (2) the focal

height curves at the focal point are similar; and (3) both colors are simultaneously recorded.

- Compare the samples to a negative control, for which no change is expected.
- Additionally, compare the data to lab recordings and in-flight recordings in steady flight. Consider that the recorded differences could be small, and the movement of the microplate from well to well could increase the signal noise.

## Funding

This study has been funded through PRODEX (ESA), the Swiss Space Office (SSO), Switzerland and the Lucerne School of Engineering and Architecture (Switzerland). The parabolic flight campaigns have been organized and funded by the European Space Agency (ESA). The funding bodies had no influence on the decision making process, study design and data interpretation.

## Data availability statement

The data is available from the corresponding author upon reasonable request.

## Author contributions

S.W. designed and built the hardware, did the study design and data analysis and prepared the figures and the manuscript. S.W., G.C., C.F., K. R., J.W. and T.B. performed the experiments. F.I. contributed to data analysis and data statistics. S.W. and M.E. provided funding. All authors reviewed the manuscript.

## Declaration of competing interest

The authors declare that they have no known competing financial interests or personal relationships that could have appeared to influence the work reported in this paper.

## Acknowledgements

We thank the European Space Agency (ESA) and Novespace (Bordeaux, France) for organizing and conducting the parabolic flight campaigns. We also thank PRODEX (ESA), the Swiss Space Office (SSO) and Lucerne School of Engineering and Architecture (Switzerland) for their financial support. We thank Cora Thiel and Oliver Ullrich from the University of Zurich (Switzerland), as well as Maik Böhmer from the Goethe University Frankfurt (Germany), for their support. We also thank the Eawag located in Kastanienbaum (Switzerland) for providing a fluorescent spectrometer. We further acknowledge Binder (Tuttlingen, Germany) for their support and the Genossenschaft Schlachthaus Ei (Sarnen, Switzerland) for providing the bovine joints. Ultimately, we thank BMG Labtech (Ortenberg, Germany) for their technical support, fruitful discussions and modifications to the plate reader.

## Appendix A. Supplementary data

Supplementary data to this article can be found online at <https://doi.org/10.1016/j.actaastro.2022.01.016>.

## References

- [1] K.L. Bennell, R.S. Hinman, A review of the clinical evidence for exercise in osteoarthritis of the hip and knee, *J. Sci. Med. Sport* 14 (2011) 4–9.
- [2] E.M. Roos, N.K. Arden, Strategies for the prevention of knee osteoarthritis, *Nature reviews, Rheumatology* 12 (2016) 92–101.
- [3] S.L. Johnston, M.R. Campbell, R. Scheuring, A.H. Feiveson, Risk of herniated nucleus pulposus among U.S. astronauts, *Aviat Space Environ. Med.* 81 (2010) 566–574.

- [4] J. Fitzgerald, Cartilage breakdown in microgravity—a problem for long-term spaceflight? *NPJ Reg. Med.* 2 (2017) 10.
- [5] V. Ramachandran, R. Wang, S.S. Ramachandran, A.S. Ahmed, K. Phan, E. L. Antonsen, Effects of spaceflight on cartilage: implications on spinal physiology, *J. Spine Surgery* 4 (2018) 433–445.
- [6] J.A. Buckwalter, V.C. Mow, A. Ratcliffe, Restoration of injured or degenerated articular cartilage, *J. Am. Acad. Orthop. Surg.* 2 (1994) 192–201.
- [7] T.M. Haqqi, D.D. Anthony, C.J. Malemud, Chondrocytes, in: G.C. Tsokos (Ed.), *Principles of Molecular Rheumatology*, Humana Press, Totowa, NJ, 2000, pp. 267–277.
- [8] M. Ulrich-Vinther, M.D. Maloney, E.M. Schwarz, R. Rosier, R.J. O’Keefe, Articular cartilage biology, *JAAOS-J. Am. Aca. Orthopaedic Surgeons* 11 (2003) 421–430.
- [9] H. Akkiraju, A. Nohe, Role of chondrocytes in cartilage formation, progression of osteoarthritis and cartilage regeneration, *J. Dev. Biol.* 3 (2015) 177–192.
- [10] A. Mobasher, S.D. Carter, P. Martin-Vasallo, M. Shakibaei, Integrins and stretch activated ion channels; putative components of functional cell surface mechanoreceptors in articular chondrocytes, *Cell Biol. Int.* 26 (2002) 1–18.
- [11] S. Grad, D. Eglin, M. Alini, M.J. Stoddart, Physical stimulation of chondrogenic cells in vitro: a review, *Clin. Orthop. Relat. Res.* 469 (2011) 2764–2772.
- [12] D.E. Anderson, B. Johnstone, Dynamic mechanical compression of chondrocytes for tissue engineering: a critical review, *Front. Bioeng. Biotechnol.* 5 (2017) 76.
- [13] Z. Zhao, Y. Li, M. Wang, S. Zhao, Z. Zhao, J. Fang, Mechanotransduction pathways in the regulation of cartilage chondrocyte homeostasis, *J. Cell Mol. Med.* 24 (2020) 5408–5419.
- [14] A. Anishkin, S.H. Loukin, J. Teng, C. Kung, Feeling the hidden mechanical forces in lipid bilayer is an original sense, *Proc. Natl. Acad. Sci. U. S. A.* 111 (2014) 7898–7905.
- [15] J. Arnodottir, M. Chalfie, Eukaryotic mechanosensitive channels, *Annu. Rev. Biophys.* 39 (2010) 111–137.
- [16] O.P. Hamill, B. Martinac, Molecular basis of mechanotransduction in living cells, *Physiol. Rev.* 81 (2001) 685–740.
- [17] F. Sachs, Stretch-activated ion channels: what are they? *Physiology* 25 (2010) 50–56.
- [18] P.G. Gillespie, R.G. Walker, Molecular basis of mechanosensory transduction, *Nature* 413 (2001) 194–202.
- [19] J. Parvizi, V. Parpura, J.F. Greenleaf, M.E. Bolander, Calcium signaling is required for ultrasound-stimulated aggrecan synthesis by rat chondrocytes, *J. Orthop. Res. : Official Pub. Orthopaedic Res. Soc.* 20 (2002) 51–57.
- [20] J.K. Mouw, S.M. Imler, M.E. Levenston, Ion-channel regulation of chondrocyte matrix synthesis in 3D culture under static and dynamic compression, *Biomech. Model. Mechanobiol.* 6 (2007) 33–41.
- [21] S.V. Eleswarapu, K.A. Athanasiou, TRPV4 channel activation improves the tensile properties of self-assembled articular cartilage constructs, *Acta Biomater.* 9 (2013) 5554–5561.
- [22] C.J. O’Conor, H.A. Leddy, H.C. Benefield, W.B. Liedtke, F. Guilak, TRPV4-mediated mechanotransduction regulates the metabolic response of chondrocytes to dynamic loading, *Proc. Natl. Acad. Sci. U. S. A.* 111 (2014) 1316–1321.
- [23] A.L. McNulty, H.A. Leddy, F. Guilak, TRPV4 as a therapeutic target for joint diseases, *Naunyn-Schmiedeberg’s Arch. Pharmacol.* 388 (2015) 437–450.
- [24] A. Dasca, R. Korenstein, Y. Oron, Z. Nevo, A hyperosmotic stimulus regulates intracellular pH, calcium, and S-100 protein levels in avian chondrocytes, *Biochem. Biophys. Res. Commun.* 227 (1996) 368–373.
- [25] G.R. Erickson, L.G. Alexopoulos, F. Guilak, Hyper-osmotic stress induces volume change and calcium transients in chondrocytes by transmembrane, phospholipid, and G-protein pathways, *J. Biomech.* 34 (2001) 1527–1535.
- [26] C.E. Yellowley, J.C. Hancox, H.J. Donahue, Effects of cell swelling on intracellular calcium and membrane currents in bovine articular chondrocytes, *J. Cell. Biochem.* 86 (2002) 290–301.
- [27] J.C. Sanchez, T.A. Danks, R.J. Wilkins, Mechanisms involved in the increase in intracellular calcium following hypotonic shock in bovine articular chondrocytes, *Gen. Physiol. Biophys.* 22 (2003) 487–500.
- [28] J.C. Sanchez, R.J. Wilkins, Changes in intracellular calcium concentration in response to hypertonicity in bovine articular chondrocytes, *Comparative biochemistry and physiology, Part A, Molecular & integrative physiology* 137 (2004) 173–182.
- [29] P.H. Chao, A.C. West, C.T. Hung, Chondrocyte intracellular calcium, cytoskeletal organization, and gene expression responses to dynamic osmotic loading, *Am. J. Physiol. Cell Physiol.* 291 (2006) C718–C725.
- [30] M.N. Phan, H.A. Leddy, B.J. Votta, S. Kumar, D.S. Levy, D.B. Lipschutz, S.H. Lee, W. Liedtke, F. Guilak, Functional characterization of TRPV4 as an osmotically sensitive ion channel in porcine articular chondrocytes, *Arthritis Rheum.* 60 (2009) 3028–3037.
- [31] C.E. Yellowley, C.R. Jacobs, Z. Li, Z. Zhou, H.J. Donahue, Effects of fluid flow on intracellular calcium in bovine articular chondrocytes, *Am. J. Physiol.* 273 (1997) C30–C36.
- [32] W. Lee, H.A. Leddy, Y. Chen, S.H. Lee, N.A. Zelenski, A.L. McNulty, J. Wu, K. N. Beicker, J. Coles, S. Zauscher, J. Grandl, F. Sachs, F. Guilak, W.B. Liedtke, Synergy between Piezo1 and Piezo2 channels confers high-strain mechanosensitivity to articular cartilage, *Proc. Natl. Acad. Sci. U. S. A.* 111 (2014) E5114–E5122.
- [33] P. D’Andrea, F. Vittur, Propagation of intercellular Ca<sup>2+</sup> waves in mechanically stimulated articular chondrocytes, *FEBS Lett.* 400 (1997) 58–64.
- [34] F. Guilak, R.A. Zell, G.R. Erickson, D.A. Grande, C.T. Rubin, K.J. McLeod, H. J. Donahue, Mechanically induced calcium waves in articular chondrocytes are inhibited by gadolinium and amiloride, *J. Orthop. Res. : Official Pub. Orthopaedic Res. Soc.* 17 (1999) 421–429.
- [35] T. Ohashi, M. Hagiwara, D.L. Bader, M.M. Knight, Intracellular mechanics and mechanotransduction associated with chondrocyte deformation during pipette aspiration, *Biorheology* 43 (2006) 201–214.
- [36] D.M. Salter, S.J. Millward-Sadler, G. Nuki, M.O. Wright, Integrin-interleukin-4 Mechanotransduction Pathways in Human Chondrocytes, *Clinical orthopaedics and related research*, 2001, pp. S49–S60.
- [37] J. Pietsch, J. Bauer, M. Egli, M. Infanger, P. Wise, C. Ulbrich, D. Grimm, The effects of weightlessness on the human organism and mammalian cells, *Curr. Mol. Med.* 11 (2011) 350–364.
- [38] C. Nickerson, N.R. Pellis, C.M. Ott, Effect of Spaceflight and Spaceflight Analogue Culture on Human and Microbial Cells, Springer, 2015.
- [39] F.P.M. Kohn, R. Ritzmann, Gravity and Neuronal Adaptation, in *Vitro and in Vivo-From Neuronal Cells up to Neuromuscular Responses: a First Model*, Eur Biophys J, 2017.
- [40] S.L. Wuest, B. Gantenbein, F. Ille, M. Egli, Electrophysiological experiments in microgravity: lessons learned and future challenges, *NPJ Microgravity* 4 (2018) 7.
- [41] A. Bairoch, *Cellulosaurus Micro-review 1: Cellonauts, Spacefaring Cell Lines*, OSF Preprints, 2019.
- [42] F.P.M. Kohn, High throughput fluorescent screening of membrane potential and intracellular calcium concentration under variable gravity conditions, *Microgravity Sci. Technol.* 25 (2013) 113–120.
- [43] J. Hauslage, M. Abbrecht, L. Hanke, R. Hemmersbach, C. Koch, W. Hanke, F.P. M. Kohn, Cytosolic calcium concentration changes in neuronal cells under clinorotation and in parabolic flight missions, *Microgravity Sci. Technol.* 28 (2016) 633–638.
- [44] N. Hausmann, S. Fengler, A. Hennig, M. Franz-Wachtel, R. Hampp, M. Neef, Cytosolic calcium, hydrogen peroxide and related gene expression and protein modulation in Arabidopsis thaliana cell cultures respond immediately to altered gravitation: parabolic flight data, *Plant Biol.* 16 (Suppl 1) (2014) 120–128.
- [45] M. Neef, M. Ecker, R. Hampp, Real-time recording of cytosolic calcium levels in Arabidopsis thaliana cell cultures during parabolic flights, *Microgravity Sci. Technol.* 27 (2015) 305–312.
- [46] M.B. Goldring, J.R. Birkhead, L.F. Suen, R. Yamin, S. Mizuno, J. Glowacki, J. L. Arbiser, J.F. Apperley, Interleukin-1 beta-modulated gene expression in immortalized human chondrocytes, *J. Clin. Invest.* 94 (1994) 2307–2316.
- [47] M.B. Goldring, Immortalization of human articular chondrocytes for generation of stable, differentiated cell lines, *Methods Mol. Med.* 100 (2004) 23–36.
- [48] S.L. Wuest, M. Calio, T. Wernas, S. Tanner, C. Giger-Lange, F. Wyss, F. Ille, B. Gantenbein, M. Egli, Influence of mechanical unloading on articular chondrocyte dedifferentiation, *Int. J. Mol. Sci.* 19 (2018).
- [49] V. Pletser, S. Rouquette, U. Friedrich, J.-F. Clervoy, T. Gharib, F. Gai, C. Mora, The first European parabolic flight campaign with the Airbus A310 ZERO-G, *Microgravity Sci. Technol.* 28 (2016) 587–601.
- [50] V. Pletser, Y. Kumei, Parabolic flights, in: D.A. Beysens, J.J.W.A. van Loon (Eds.), *Generation and Applications of Extra-terrestrial Environments on Earth*, River Publishers, 2015, pp. 61–73.
- [51] F. Karmali, M. Shelhamer, The dynamics of parabolic flight: flight characteristics and passenger percepts, *Acta Astronaut.* 63 (2008) 594–602.
- [52] K. von der Mark, V. Gaus, H. von der Mark, P. Muller, Relationship between cell shape and type of collagen synthesised as chondrocytes lose their cartilage phenotype in culture, *Nature* 267 (1977) 531–532.
- [53] S. Marlovits, M. Hombauer, M. Truppe, V. Vecsei, W. Schlegel, Changes in the ratio of type-I and type-II collagen expression during monolayer culture of human chondrocytes, *J. Bone Joint Surg Br* 86 (2004) 286–295.
- [54] J. Diaz-Romero, J.P. Gaillard, S.P. Grogan, D. Nestic, T. Trub, P. Mainil-Varlet, Immunophenotypic analysis of human articular chondrocytes: changes in surface markers associated with cell expansion in monolayer culture, *J. Cell. Physiol.* 202 (2005) 731–742.
- [55] J. Diaz-Romero, D. Nestic, S.P. Grogan, P. Heini, P. Mainil-Varlet, Immunophenotypic changes of human articular chondrocytes during monolayer culture reflect bona fide dedifferentiation rather than amplification of progenitor cells, *J. Cell. Physiol.* 214 (2008) 75–83.
- [56] A. Tekari, R. Luginbuehl, W. Hofstetter, R.J. Egli, Chondrocytes expressing intracellular collagen type II enter the cell cycle and co-express collagen type I in monolayer culture, *J. Orthop. Res. : Official Pub. Orthopaedic Res. Soc.* 32 (2014) 1503–1511.
- [57] M. Wright, P. Jobanputra, C. Bavington, D.M. Salter, G. Nuki, Effects of intermittent pressure-induced strain on the electrophysiology of cultured human chondrocytes: evidence for the presence of stretch-activated membrane ion channels, *Clin. Sci. (Lond.)* 90 (1996) 61–71.
- [58] S.J. Millward-Sadler, M.O. Wright, H. Lee, H. Caldwell, G. Nuki, D.M. Salter, Altered electrophysiological responses to mechanical stimulation and abnormal signalling through alpha5beta1 integrin in chondrocytes from osteoarthritic cartilage, *Osteoarthritis and cartilage/OARS, Osteoarthritis Res. Soc.* 8 (2000) 272–278.
- [59] L. Ramage, M.A. Martel, G.E. Hardingham, D.M. Salter, NMDA receptor expression and activity in osteoarthritic human articular chondrocytes, *Osteoarthritis and cartilage/OARS, Osteoarthritis Res. Soc.* 16 (2008) 1576–1584.
- [60] Q.Q. Wu, Q. Chen, Mechanoregulation of chondrocyte proliferation, maturation, and hypertrophy: ion-channel dependent transduction of matrix deformation signals, *Exp. Cell Res.* 256 (2000) 383–391.
- [61] S.J. Bonvini, M.A. Birrell, E. Dubuis, J.J. Adcock, M.A. Wortley, P. Flajolet, P. Bradding, M.G. Belvisi, Novel airway smooth muscle-mast cell interactions and a role for the TRPV4-ATP axis in non-atopic asthma, *Eur. Respir. J.* 56 (2020).
- [62] E. Isoya, F. Toyoda, S. Imai, N. Okumura, K. Kumagai, M. Omatsu-Kanbe, M. Kubo, H. Matsuura, Y. Matsusue, Swelling-activated Cl(-) current in isolated rabbit

articular chondrocytes: inhibition by arachidonic Acid, *J. Pharmacol. Sci.* 109 (2009) 293–304.

- [63] S. Muramatsu, M. Wakabayashi, T. Ohno, K. Amano, R. Ooishi, T. Sugahara, S. Shiojiri, K. Tashiro, Y. Suzuki, R. Nishimura, S. Kuhara, S. Sugano, T. Yoneda, A. Matsuda, Functional gene screening system identified TRPV4 as a regulator of chondrogenic differentiation, *J. Biol. Chem.* 282 (2007) 32158–32167.
- [64] M. Grandolfo, M. Martina, F. Ruzzier, F. Vittur, A potassium channel in cultured chondrocytes, *Calcif. Tissue Int.* 47 (1990) 302–307.
- [65] J.W. Mozrzymas, M. Martina, F. Ruzzier, A large-conductance voltage-dependent potassium channel in cultured pig articular chondrocytes, *Pflügers Archiv* 433 (1997) 413–427.
- [66] L.M. Loew, Design and use of organic voltage sensitive dyes, in: M. Canepari, D. Zecevic (Eds.), *Membrane Potential Imaging in the Nervous System: Methods and Applications*, Springer New York, New York, NY, 2011, pp. 13–23.
- [67] A. Hammer, G. Cerretti, D.A. Ricciardi, D. Schiffmann, S. Maranda, R. Kummer, C. Zumbühl, K.F. Rattenbacher-Kiser, S. von Arx, S. Ammann, F. Strobl, R. Berkane, A. Stolz, E.H.K. Stelzer, M. Egli, E. Schleiff, S.L. Wuest, M. Böhmer, Retrograde Analysis of Calcium Signaling by CaMPARI2 Shows Cytosolic Calcium in Chondrocytes Is Unaffected by Parabolic Flights 10, *Biomedicines*, 2022, p. 138.
- [68] S.B. Hastie, Interactions of colchicine with tubulin, *Pharmacol. Ther.* 51 (1991) 377–401.
- [69] S.L. Wuest, J. Arnold, S. Gander, C. Zumbühl, C. Jost, C. Giger-Lange, G. Cerretti, M. Caliò, K. Rattenbacher-Kiser, C. Follonier, O. Schälli, G.S. Székely, M. Egli, F. Ille, Microtubules and vimentin fiber stability during parabolic flights, *Microgravity Sci. Technol.* 32 (2020) 921–933.
- [70] P.M.F. Kohn, High throughput fluorescent screening of membrane potential under variable gravity conditions, in: *Life in Space for Life on Earth*, European Space Agency, Aberdeen, UK, 2012.



Cindy Follonier obtained her PhD in molecular biology from the University of Zurich in 2012. Her award winning PhD project focused on the expansion of trinucleotide repeats involved in Friedreich's ataxia. She then joined Princeton University in the USA for a postdoc position, where she studied the functions of the helicase PIF1, in human cells. In 2018, she came back to Switzerland and joined the Lucerne School of Engineering and Architecture (Hochschule Luzern) as Payload Operations Engineer for BIOTESC (Biotechnology Space Support Center) and also contributed to research projects of the Institute of Medical Engineering.



Karin Rattenbacher-Kiser is currently a research assistant at the Institute of Medical Engineering at the Lucerne School of Engineering and Architecture (Hochschule Luzern). After she studied Biology at the University of Basel, Switzerland, she worked at the Institute for Medical Microbiology at the University of Basel. Her research topics involved the characterization of mast cell mutants acquiring sensitivity to the drug rapamycin. She continued her studies in the department of Microbiology at the University of Minnesota, Minneapolis, USA, where she worked on mRNA stability of T lymphocytes.



Simon Wüest is a post-doc research associate at the Institute of Medical Engineering at the Lucerne School of Engineering and Architecture (Hochschule Luzern). His research interests cover the influence of gravity on biological systems (gravitational biology) and how cells respond to their mechanical environment (cellular mechanosensation). Participation in several parabolic flight campaigns and a sounding rocket mission highlight his career. Besides conducting basic research in zero gravity, he also enjoys developing the required scientific instrumentation. Simon Wüest studied Systems Engineering and subsequently Biomedical Engineering. He received his PhD in Biomedical Engineering from the University of Bern.



Timothy Bradley is pursuing a Master's degree in systems biology at the Swiss Federal Institute of Technology in Zurich (ETHZ). His research projects have focused on metabolic and protein engineering within the framework of a sustainable circular bioeconomy. Since the end of 2019, he has been a member of the data analysis team in the group of Prof. Oliver Ullrich at the University of Zurich's Division of Space Life Sciences and Gravitational Biology, where he is contributing towards a multi-omics approach to elucidate the effects of altered gravity on human immune cells.



Geraldine Cerretti is currently a research assistant at the Institute of Medical Engineering at the Lucerne School of Engineering and Architecture (Hochschule Luzern), supporting various research projects for the Space Biology Group. She studied Biotechnology at the ESBS (École Supérieure de Biotechnologie de Strasbourg, France) and completed her Master's project at the QIMR Berghofer Medical Research Institute (Brisbane, Australia) in 2010. She then worked several years at the IMB (Institute for Molecular Bioscience, The University of Queensland) before moving back to Switzerland in 2016. She joined the Space Biology Group in 2018 after having worked at the University of Bern.



Marcel Egli is head of the Institute of Medical Engineering at the Lucerne University of Applied Sciences and Arts and the National Centre for Biomedical Research in Space at the Innovation Cluster Space and Aviation (Space Hub) of the University of Zurich. He has published numerous papers in the fields of neuro-endocrinology and space biology. His current research interest is focused on the cellular basis of mechanosensation. By using research platforms like airplanes performing parabolic flights, sounding rockets, and the International Space Station, questions like how cells behave in a mechanically unloaded environment of microgravity are addressed.



Jennifer Wadsworth is a microbiologist specializing in radiation biology. She received her BSc in Biology from the University of Basel and went on to receive her PhD in Physics at the University of Edinburgh focusing on microbes under extreme radiation conditions. After completing her degree she was awarded a NASA Postdoctoral Research Fellowship and continued her research at the NASA Ames Research Center, California, working on developing new clean room sterilization techniques. She is currently working as a research associate at the Institute of Medical Engineering, Lucerne School of Engineering and Architecture (Hochschule Luzern) and is also lecturing a masters-level course on life detection at the University of Zürich.



Fabian Ille is head of the Competence Center for Bioscience and Medical Engineering at the Lucerne School of Engineering and Architecture (Hochschule Luzern), Institute of Medical Engineering. He has published numerous papers in the fields of reproductive and cell biology. His current research interest is focused on the effects microgravity on joint and intervertebral disk degeneration and regeneration processes. He combines microgravity experiments with multi omics approaches to address cell differentiation processes under simulated and real microgravity.